Topotactic Hydrogen in Nickelate Superconductors and Akin Infinite-Layer Oxides ABO_2

Liang Si,[1,2] Wen Xiao,[1] Josef Kaufmann,[2] Jan M. Tomczak,[2] Yi Lu,[3] Zhicheng Zhong,[1,4,*] and Karsten Held[2,†]

[1]*Key Laboratory of Magnetic Materials and Devices and Zhejiang Province Key Laboratory of Magnetic Materials and Application Technology, Ningbo Institute of Materials Technology and Engineering (NIMTE), Chinese Academy of Sciences, Ningbo 315201, China*

[2]*Institute for Solid State Physics, Vienna University of Technology, 1040 Vienna, Austria*

[3]*Institute for Theoretical Physics, Heidelberg University, Philosophenweg 19, 69120 Heidelberg, Germany*

[4]*China Center of Materials Science and Optoelectronics Engineering, University of Chinese Academy of Sciences, Beijing 100049, China*

(Received 15 November 2019; accepted 1 April 2020; published 22 April 2020)

Superconducting nickelates appear to be difficult to synthesize. Since the chemical reduction of ABO_3 [rare earth (A), transition metal (B)] with CaH_2 may result in both ABO_2 and ABO_2H, we calculate the topotactic H binding energy by density functional theory (DFT). We find intercalating H to be energetically favorable for $LaNiO_2$ but not for Sr-doped $NdNiO_2$. This has dramatic consequences for the electronic structure as determined by DFT + dynamical mean field theory: that of $3d^9$ $LaNiO_2$ is similar to (doped) cuprates, $3d^8$ $LaNiO_2H$ is a two-orbital Mott insulator. Topotactic H might hence explain why some nickelates are superconducting and others are not.

DOI: 10.1103/PhysRevLett.124.166402

Most recently superconductivity was found in $Nd_{0.8}Sr_{0.2}NiO_2$ films grown on $SrTiO_3$ [1], a seminal work that opens the door wide to a new age of superconductivity: the nickelate age. These novel (Sr-doped) $NdNiO_2$ superconductors are not only isostructural to the well-known cuprate superconductor $CaCuO_2$ [2–5], but also both Ni and Cu are formally $3d^9$ in the respective parent compound.

Strikingly different to the cuprates [6] and iron pnictides [7], reproducing these outstanding results in isoelectronic compositions appears to be quite challenging. In a more bulklike crystal, no superconductivity was reported for $Nd_{0.8}Sr_{0.2}NiO_2$ [8], nor when directly pulsed laser depositing $Nd_{0.8}Sr_{0.2}NiO_x$ [9]. Also the parent compound $NdNiO_2$ is not superconducting [1], but shows a resistivity upturn toward low temperatures. Another nickelate, $LaNiO_2$, is also isostructural and isovalent, but is a (bad) metal [10] with neither superconductivity, nor antiferromagnetism [11].

An obvious difference between $Nd_{0.8}Sr_{0.2}NiO_2$ and $Nd(La)NiO_2$ is doping. However, in contrast to the cuprates, there is already a self-doping of the Ni bands in $Nd(La)NiO_2$ because one Nd(La) band crosses the Fermi energy [12–15], hardly hybridizing with the Ni $3d_{x^2-y^2}$ bands. Why are some of these nickelates, all of which have a similar paramagnetic (spin-unpolarized) density functional theory (DFT) electronic structure [12–14,16–28], superconducting but others are not?

Let us take a step back and recapitulate the synthesis of $ANiO_2$ nickelates with the unusual low oxidation state Ni^+. It is synthesized by first growing $ANiO_3$ on a $SrTiO_3$ substrate and then reducing it to $ANiO_2$ with the help of the reagent CaH_2, see Fig. 1. However, there is another possible end product: $ANiO_2H$. Indeed, for another perovskite, $SrVO_3$, it was shown in a detailed experimental analysis [29] that the CaH_2 reduction reaction leads to $SrVO_2H$; also $NdNiO_xH_y$ has been detected [30].

In this Letter, we show, based on DFT calculations [31–33], that the nickelates are just at the borderline of the two reaction paths of Fig. 1: While for $A = Nd$ and, in particular, for $A = La$, the oxide-hydrides $NdNiO_2H$ and $LaNiO_2H$ are energetically favorable, with Sr doping, the

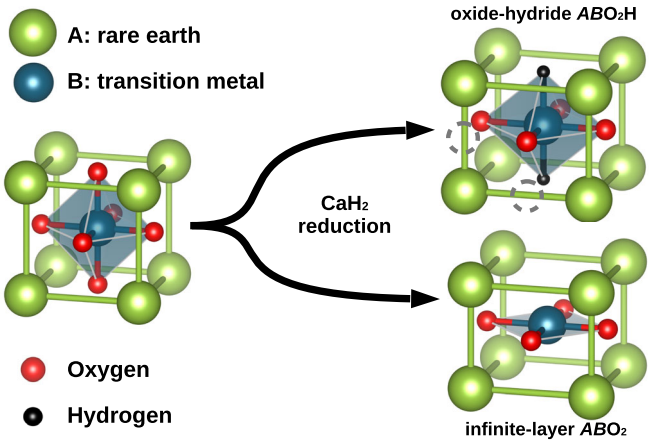

FIG. 1. Two possible products in the topotactic reduction of ABO_3 by means of CaH_2: oxide-hydride ABO_2H and infinite-layer ABO_2. The dashed circles indicate other possible H positions for ABO_2H, which are, however, energetically less favorable.

infinite-layer $Nd_{0.8}Sr_{0.2}NiO_2$ becomes more stable. As a matter of course, the reaction kinetics also influences the end products, and without carefully optimizing the reaction conditions, some mixed phase of $ANiO_2$ and $ANiO_2H$ may emerge. We further demonstrate that the H intercalation has dramatic consequences for the electronic structure as calculated by DFT and DFT + dynamical mean field theory (DMFT) [34–37]: While $ANiO_2$ is metallic with a very strong quasiparticle renormalization of the Ni $d_{x^2-y^2}$ band and Nd(La)-5d pocket, quite similar to doped cuprates, $ANiO_2H$ is a Mott insulator with two Ni bands, $d_{x^2-y^2}$ and d_{z^2}, and no Nd(La)-5d pocket.

Methods.—Structural details and H-topotactic binding energies are computed by DFT structural relaxations (yielding lattice constants $a = b = 3.889$, $c = 3.337$ Å for $LaNiO_2$, and $a = b = 3.914$, $c = 3.383$ Å for $LaNiO_2H$) and total energy calculations. Both WIEN2K [38,39] and Vienna *ab initio* simulation package (VASP) [40] codes within Perdew-Burke-Ernzerhof (PBE) [41] and PBE-sol [42] versions of the generalized gradient approximation (GGA) are employed on a $13 \times 13 \times 15$ momentum grid. The energy cutoff was 500 eV in VASP; $R_{MT}K_{max} = 7.0$ with a muffin-tin radius $R_{MT} = 2.50$, 1.96, 1.69, and 1.10 a.u. for La, Ni, O, and H, respectively, was employed in WIEN2K.

For the DMFT calculations, the WIEN2K band structure around the Fermi level is projected onto Wannier functions [43,44] using WIEN2WANNIER [45,46] and supplemented by a local density-density interaction, taking the fully localized limit [47] as double counting. Since for infinite-layer $LaNiO_2$, La-d bands cross the Fermi level E_F, here a full set of La-5d + Ni-3d bands is adopted. For $LaNiO_2H$, a projection onto the Ni-3d bands is possible only because now the La-5d bands are well separated from the Ni-3d bands (cf. Supplemental Material [48] for La-d bands included in DMFT). The interaction parameters are computed by constrained random phase approximation [49]: average interorbital interaction $U' = 3.10$ eV (2.00) and Hund's exchange $J = 0.65$ eV (0.25) for Ni (La). The intraorbital Hubbard interaction follows as $U = U' + 2J$. These interaction parameters are close to those of previous studies [50,51] for 3d oxides. The resulting Hamiltonian is then solved at room temperature (300 K) in DMFT using continuous-time quantum Monte Carlo simulations in the hybridization expansions [52] implemented in W2DYNAMIC [53,54]; the maximum entropy method [55,56] is employed for an analytic continuation of the spectra.

Energetics of topotactic hydrogen.—In addition to the two cornerstone end products, infinite-layer ABO_2 (e.g., $CaCuO_2$, $SrCuO_2$) and oxide-hydride ABO_2H (e.g., $SrVO_2H$) of Fig. 1, and also intermediate products such as $(Ba, Sr, Ca)TiO_{3-x}H_x$ [57,58] and $NdNiO_xH_y$ [30] have been experimentally confirmed when reducing ABO_3 with CaH_2 upon heating [59,60]. To investigate whether it is energetically favorable to intercalate hydrogen in the topotactic reaction or not, we compute the hydrogen binding energy

$$E_B = E[ABO_2] + \mu[\mathrm{H}] - E[ABO_2\mathrm{H}]. \tag{1}$$

Here, $E[ABO_2]$ and $E[ABO_2H]$ are the total energy of ABO_2 and ABO_2H; and $\mu[\mathrm{H}] = E[\mathrm{H}_2]/2$ is the chemical potential of H. Note that H_2 is a typical byproduct for the reduction with CaH_2 and also emerges when CaH_2 is in contact with H_2O. Hence, it can be expected to be present in the reaction. E_B is also the difference in binding energy for the two reaction paths of Fig. 1; i.e., it is energetically favorable by E_B to synthesize ABO_2H instead of ABO_2 and $H_2/2$. Of course, the reaction kinetics may change the outcome and the large entropy of $1/2$ H_2 might change the balance thermodynamically in favor of ABO_2 [63]. However, at the very least, the energetics gives us a first hint whether to expect ABO_2H or ABO_2.

As for the three H positions of Fig. 1, we always find that the vacancy left by the removed oxygen is the energetically favored H position. For a full H-topotactic intercalation, i.e., ABO_2H with all vacant oxygen positions occupied by H, this is plotted explicitly in Fig. 1. We first consider this complete intercalation, fully relax the ABO_2 and ABO_2H structures, and then calculate the respective total spin-unpolarized DFT energy and from this E_B through Eq. (1). Our conclusions remain unchanged when using spin-polarized DFT + U instead, see Supplemental Material [48].

For $SrBO_2$ and $LaBO_2$, E_B is positive from Ti to Co in Fig. 2(a), indicating the energetical preference for the oxide-hydride $SrBO_2H$ for $B = \mathrm{Ti}, \ldots, \mathrm{Co}$. This is consistent with finding $SrVO_2H$ and $SrTiO_xH_y$ after CaH_2 reduction [29,65–67]. Similarly, oxide-hydrides have been reported experimentally when reducing $(Sr, La)CoO_3$ [68,69] and $(Ba, Ca, Sr)TiO_3$ [58,70,71].

Surprisingly, for $LaNiO_2$, a positive E_B of 0.162 eV is predicted, too. This indicates incorporating H topotactically in infinite-layer $LaNiO_2$ is at least energetically favorable. For $SrNiO_2$, on the other hand, it is energetically unfavorable to intercalate H. That is, the nickelates $ANiO_2$ are just at the borderline $E_B = 0$ in Fig. 2(a); the cation A is decisive. The cuprates, on the other hand, are clearly on the $E_B < 0$ side; i.e., hydrogen will not be intercalated, consistent with the well-studied chemistry of the cuprates.

Besides the La- and Sr-based infinite-layer ABO_2, we also calculate E_B for a few additional materials: $CaCuO_2$ [2] has $E_B < 0$ as the other cuprate superconductors, and undoped $NdNiO_2$ [72] has $E_B = 0.133$ eV, which turns negative to $E_B = -0.113$ eV if 25% of Nd atoms are replaced by Sr. Hence, our results indicate that infinite-layer, superconducting Sr-doped $NdNiO_2$ is energetically stable against the topotactic inclusion of H, whereas other nickelates are not.

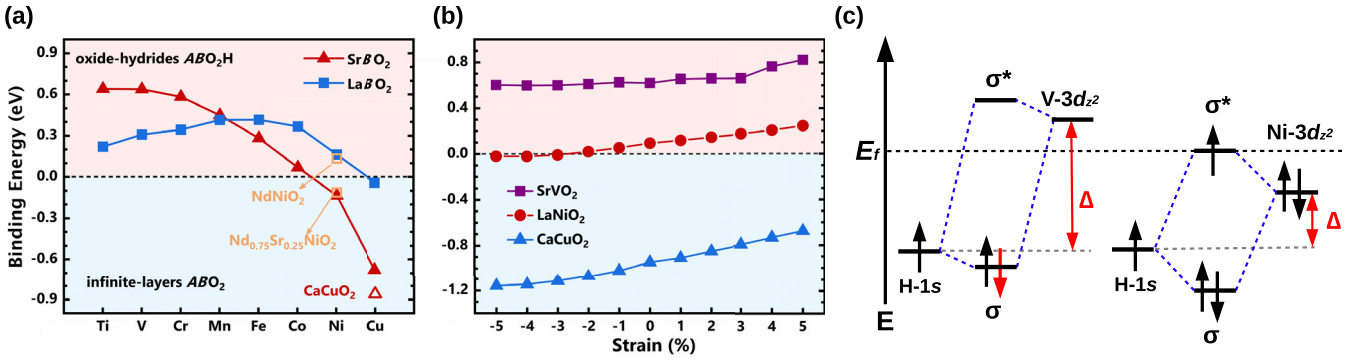

FIG. 2. (a) Binding energy E_B for topotactic H in infinite-layer ABO_2 [Sr or La (A), Ti to Cu (B)]. Further, E_B for $CaCuO_2$, $NdNiO_2$, and $Nd_{0.75}Sr_{0.25}NiO_2$ is plotted. (b) E_B for $SrVO_2$, $LaNiO_2$, and $CaCuO_2$ as a function of strain at a low H density of 12.5%. (c) Explanation of the evolution of the H-topotactic binding energy from AVO_2 to $ANiO_2$ based on the formation of bonding (σ) and antibonding (σ^*) states between H-1 s and transition metal $3d_{z^2}$. The up and down arrows indicate the electron spins; the red arrow for AVO_2 means the electron is from other (V-t_{2g}) orbitals.

The complete (full) topotactic inclusion of H, where all vacancies induced by removing oxygen are filled by H, is an ideal limiting case. Under varying experimental conditions, such as chemical reagent, substrate, temperature, and strain, the H-topotactic inclusion may be incomplete, and ABO_2H_y ($y < 1$) energetically favored. Hence, we also compute E_B at a rather low H-topotactic density: $ABO_2H_{0.125}$ (achieved by including a single H into $2 \times 2 \times 2$ ABO_2 supercells). Additionally, we model strain effects by changing the in-plane lattice constants (a, b) and relaxing the lattice in the z direction and the internal atomic positions.

Figure 2(b) shows the corresponding E_B for $SrVO_2H_{0.125}$, $LaNiO_2H_{0.125}$, and $CaCuO_2H_{0.125}$. Unstrained (0%), the binding energy E_B per hydrogen (0.620 eV for $SrVO_2H_{0.125}$, 0.094 eV for $LaNiO_2H_{0.125}$, and -0.945 eV for $CaCuO_2H_{0.125}$) is very similar to complete hydrogen intercalation ($E_B = 0.637$ eV for $SrVO_2H$, 0.162 eV for $LaNiO_2H$, and -0.859 eV for $CaCuO_2H$) in Fig. 2(a). This indicates that the topotactic intercalation with H does not depend too much on the amount of H. Figure 2(b) further shows that E_B is substantially reduced by compressive (negative) strain. This is because the compressive strain enlarges the z axis, which in turn leads to weaker H-B-H bonding. This suggests compression to be an effective way to eliminate residual H in $ANiO_2$. It might also explain why $NdNiO_2$ was found next to the interface of (compressive) $SrTiO_3$, whereas $NdNiO_xH_y$ was found further away from the interface [30].

Let us now ask why E_B varies remarkably for different ABO_2. In addition to the gradually changing lattice constants, the dominating factor is the d-band filling. By computing the band characteristics (Fig. 3), we find H^- which, similar to $O^{2-}_{0.5}$, absorbs one Ni electron. For early transition metals with positive E_B, as, e.g., $SrVO_2H$, the H-1 s forms bonding (σ) and antibonding (σ^*) states due to the orbital overlap with V-d_{z^2} as sketched on the left side of Fig. 2(c). The bonding σ orbital is fully occupied with one electron originating for the H-1 s and the second from the V-t_{2g} orbitals. This explains the stabilization and energy gain of $SrVO_2H$.

For late transition metals, e.g., $LaNiO_2H$, the $3d_{z^2}$ is fully filled, see right side of Fig. 2(c). Hence, when intercalating H, the antibonding σ^* orbital also needs to be occupied with one electron and then crosses E_F. This and the smaller bonding-antibonding splitting reduces the energy gain for the topotactic intercalation of H. This puts the nickelates at the borderline, whereas for the next transition metal, Cu, it is no longer energetically favorable to form $ACuO_2H$.

Spin-unpolarized DFT electronic structure.—Let us now address the question, how much does the electronic structure change if topotactic hydrogen is present? In the infinite-layer $LaNiO_2$, the Ni $d_{x^2-y^2}$ orbital shows a single-band dispersion without hybridization with other bands, similar to the Cu-$d_{x^2-y^2}$ dispersion in cuprates. However, in contrast to the cuprates, there is an itinerant La band that crosses E_F around the A point, see Fig. 3(a) and [13–16]. It is composed of La-5d, but also La-4f and with some Ni-t_{2g} intermixing. There is no discernible hybridization gap when this La band crosses the Ni-$d_{x^2-y^2}$ band in Fig. 3(a) because of the (symmetry-dictated) very weak hybridization between both [15].

For $LaNiO_2H$, the topotactic H alters the DFT band structure completely, see Fig. 3(b). First, the La band crossing at E_F around the A point is gone. This is because the La-d_{xy} hopping in the (110) direction changes sign when connected though the H-1 s orbital: from -0.098 eV for $LaNiO_2$ to 0.224 eV for $LaNiO_2H$. This turns the minimum (La-5d pocket) around the A point in Fig. 3(a) into a maximum in Fig. 3(b). Second, the Ni-d_{z^2} band is now partially occupied for $LaNiO_2H$ instead of being fully occupied in infinite-layer $LaNiO_2$. Three factors contribute

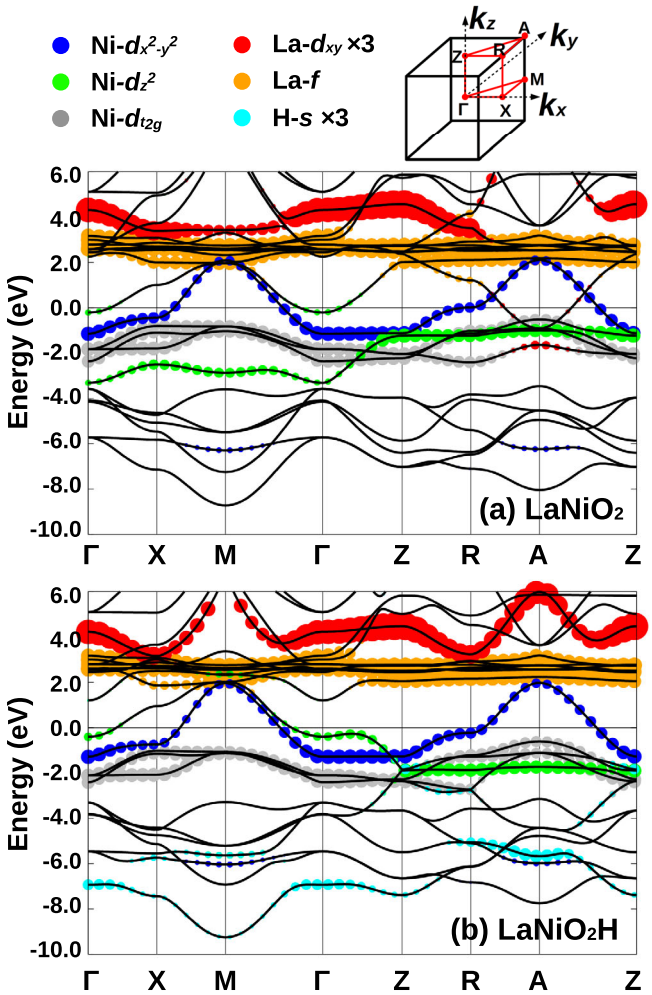

FIG. 3. DFT band structure and orbital characters for (a) $LaNiO_2$ and (b) $LaNiO_2H$ along a high symmetry path through the Brillouin zone (top).

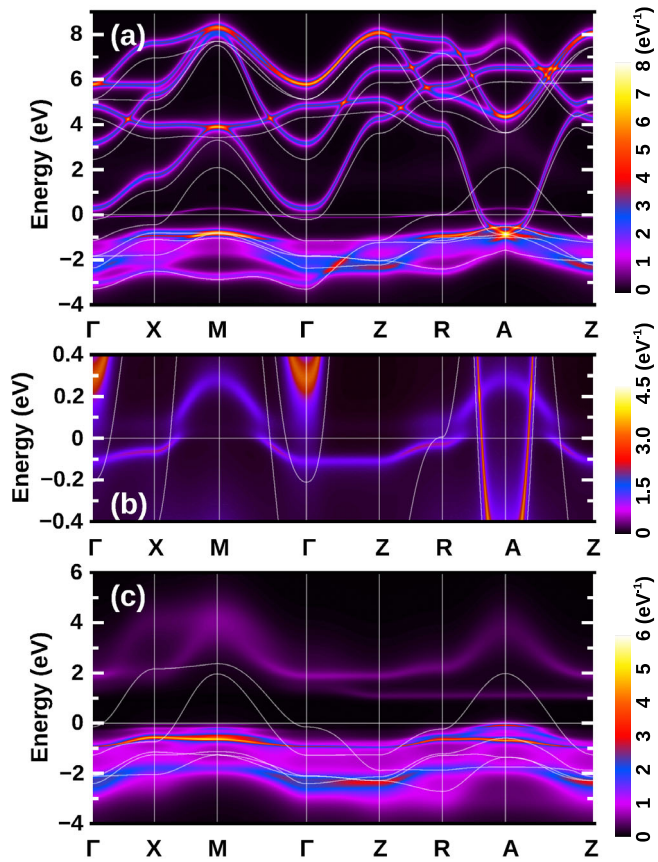

FIG. 4. DMFT spectral functions $A(k,\omega)$ of (a) $LaNiO_2$ and (c) $LaNiO_2H$; solid lines, DFT Wannier bands. (b) Enlargement of (a) around $E_F = 0$.

to this: (1) The local Ni-d_{z^2} potential is shifted up by ~1.5 eV because the d_{z^2} orbitals point toward the negatively charged H^-. (2) The intraorbital, nearest-neighbor hopping of the d_{z^2} electrons along k_z [Γ–Z in Figs. 3(a) and 3(b)] changes sign from −0.308 eV for $LaNiO_2$ to 0.781 eV for $LaNiO_2H$. (3) Last, but not least, H^- reduces the valence of Ni from Ni^{9+} to Ni^{8+}, effectively reducing E_F. Altogether, we end up in a situation that is much less akin to the cuprates: a $3d^8$ electronic configuration with two Ni orbitals, $3d_{x^2-y^2}$ and d_{z^2}, but no La-5d band around E_F.

DFT + DMFT *electronic structure*.—In transition metal oxides, we have strong effects of electronic correlations that are not properly described by the spin-unpolarized DFT band structure. One can describe the opening of a Mott-like gap by spin-polarized DFT + U (see Supplemental Material [48] and [73,74]) or by random spin orientations (or symmetry-lowering distortions) in a large supercell [75–80]. We will instead employ DFT + DMFT calculations in the paramagnetic phase at room temperature (300 K) in the following. For $LaNiO_2$ [Fig. 4(a)], electronic correlations lead to a dramatic quasiparticle renormalization Z or mass enhancement $m^*/m = 1/Z \sim 7$ of the almost half filled Ni $3d_{x^2-y^2}$ band, see enlargement in Fig. 4(b); the other Ni-3d bands are almost completely filled and below E_F. In DMFT, the La-5d band still crosses E_F around the A point, see Fig. 4(a), but the Γ pocket is lifted above E_F if we take the La-d interaction into account (cf. Supplemental Material [48]). Actually, its band dispersion hardly changes since the La-5d bands are only lightly occupied. One noteworthy effect of electronic correlations is, however, to reduce the number of holes (vs half filling) in the $3d_{x^2-y^2}$ orbital, from 0.08 per Ni site for the DFT-derived Wannier Hamiltonian to 0.03 in DMFT. Without additional doping, such a light hole doping is likely not enough to induce superconductivity.

Being so close to the Mott transition (a half filled Ni $3d_{x^2-y^2}$ band would be Mott insulating), minor modifications of the computational procedure, such as including the La-d, or changes of the experimental setup will slightly change the doping of the Ni $3d_{x^2-y^2}$ band. Even a slight change in doping will have a big effect on the quasiparticle renormalization (see Supplemental Material [48]). We think

this explains the quite substantial variation of Z in different DFT + DMFT calculations [88–91].

For the oxide-hydride $LaNiO_2H$, on the other hand, the La-5d pockets around the A point are eliminated not only in DFT [Fig. 3(b)] but also in DFT + DMFT [Fig. 4(c)]. Without doping through the La-5d pocket and the additional H^-, Ni is in an undoped $3d^8$ configuration with holes in both the d_{z^2} and $d_{x^2-y^2}$ orbitals. This integer filling of the Ni d orbitals drives $LaNiO_2H$ into a Mott insulating phase with a gap of ~0.3 eV in Fig. 4(c); a similar electronic structure for $LaNiO_2H$ can also be described by DFT + U, see Supplemental Material [48]. It is consistent with the experimental observations that $LaNiO_{2.5}$, having formally the same Ni valence, was found to be insulating [93,94]. While here we find that already the paramagnetic phase is insulating, C- or G-type antiferromagnetic ordering [95] can be expected. Similarly, $SrVO_2H$ is antiferromagnetic with a high T_N [65], whereas $SrVO_3$ is a paramagnetic metal.

Conclusion and outlook.—In another class of correlated superconductors, the iron pnictides [7,96], it is well known that hydrogen plays an important role [104], and also when using CaH_2 as a reduction reagent [105]. Here, by performing DFT and DFT + U calculations, we find that the topotactic intercalation of hydrogen in infinite-layer ABO_2 is energetically favorable for early transition metals B.

This intercalation has dramatic consequences for the electronic structures. $LaNiO_2H$ is a $3d^8$ Mott insulator with two relevant orbitals around E_F, $3d_{z^2}$ and $3d_{x^2-y^2}$, but no La-5d pockets: A situation that is distinctively different from the cuprate superconductors. Indeed, this two-orbital situation bears some similarities to $LaNiO_3/LaAlO_3$ heterostructures prior to engineering their band structure to a cupratelike one [106–111]. On the other hand, $LaNiO_2$ with a $3d^9$ configuration and the holes only in the $d_{x^2-y^2}$ orbital closely resembles the band structure of the doped cuprates. This $d_{x^2-y^2}$ orbital is lightly doped already for the parent compound because of a La-5d pocket around the A point.

The strikingly different susceptibility toward topotactic intercalation of hydrogen and the dramatic consequences for the electronic structure may explain why some nickelates have been found to be superconducting and others not. In addition to $La(Nd)NiO_2H$, an incomplete reduction to $La(Nd)NiO_{2.5}$ [112] will also lead to a similar Ni $3d^8$ electronic configuration, and there may be mixed phases thereof in an actual experiment. While hydrogen is difficult to detect, careful studies already confirmed its presence when reducing $SrVO_3$ [29], SmFeAsO [105], and $NdNiO_3$ [30,113,114] with the reagent CaH_2.

Our findings call for a careful reanalysis of the hydrogen content in nickelates. Further, we suggest that for synthesizing $ANiO_2$ without H and an electronic structure prone to superconductivity, compressive strain and Sr doping are an advantage, as are long reaction times for reducing the H_2 pressure and, according to [30], low temperatures. Quite a number of capping layers might be needed to stabilize the system against further hydrogen intercalation, and doping with a divalent cation such as Sr appears to be necessary to arrive in the superconductive doping regime.

We thank O. Janson, P. Hansmann, and A. Prokofiev for helpful comments and discussions. L. S., W. X., and Z. Z. gratefully acknowledge financial support from the National Key R&D Program of China (2017YFA0303602), Key Research Program of Frontier Sciences of CAS (Grant No. ZDBS-LY-SLH008), and the National Nature Science Foundation of China (11774360, 11904373). L. S., J. K., J. M. T., and K. H. were supported by the Austrian Science Fund (FWF) through Projects No. P 30997 and No. P 32044. Y. L. acknowledges support by Deutsche Forschungsgemeinschaft (DFG) under Germany's Excellence Strategy EXC2181/1-390900948 (the Heidelberg STRUCTURES Excellence Cluster). Calculations have been done on the Vienna Scientific Clusters (VSC) and the Supercomputing Center at NIMTE CAS.

Note added.—Further information on the synthesis used in Ref. [1] became recently available in Ref. [115].

*Corresponding author.
zhong@nimte.ac.cn
†Corresponding author.
held@ifp.tuwien.ac.at

[1] D. Li, K. Lee, B. Y. Wang, M. Osada, S. Crossley, H. R. Lee, Y. Cui, Y. Hikita, and H. Y. Hwang, Nature (London) **572**, 624 (2019).
[2] T. Siegrist, S. Zahurak, D. Murphy, and R. Roth, Nature (London) **334**, 231 (1988).
[3] G. Balestrino, P. G. Medaglia, P. Orgiani, A. Tebano, C. Aruta, S. Lavanga, and A. A. Varlamov, Phys. Rev. Lett. **89**, 156402 (2002).
[4] P. Orgiani, C. Aruta, G. Balestrino, D. Born, L. Maritato, P. G. Medaglia, D. Stornaiuolo, F. Tafuri, and A. Tebano, Phys. Rev. Lett. **98**, 036401 (2007).
[5] D. Di Castro, C. Cantoni, F. Ridolfi, C. Aruta, A. Tebano, N. Yang, and G. Balestrino, Phys. Rev. Lett. **115**, 147001 (2015).
[6] J. G. Bednorz and K. A. Müller, Z. Phys. B **64**, 189 (1986).
[7] Y. Kamihara, H. Hiramatsu, M. Hirano, R. Kawamura, H. Yanagi, T. Kamiya, and H. Hosono, J. Am. Chem. Soc. **128**, 10012 (2006).
[8] Q. Li, C. He, J. Si, X. Zhu, Y. Zhang, and H.-H. Wen, Commun. Mater. **1**, 16 (2020).
[9] X. Zhou, Z. Feng, P. Qin, H. Yan, S. Hu, H. Guo, X. Wang, H. Wu, X. Zhang, H. Chen, X. Qiu, and Z. Liu, Rare Metals (2020), https://doi.org/10.1007/s12598-020-01389-2.
[10] D. Kaneko, K. Yamagishi, A. Tsukada, T. Manabe, and M. Naito, Physica (Amsterdam) **469C**, 936 (2009).

[11] M. A. Hayward, M. A. Green, M. J. Rosseinsky, and J. Sloan, J. Am. Chem. Soc. **121**, 8843 (1999).
[12] G.-M. Zhang, Y.-F. Yang, and F.-C. Zhang, Phys. Rev. B **101**, 020501(R) (2020).
[13] Y. Nomura, M. Hirayama, T. Tadano, Y. Yoshimoto, K. Nakamura, and R. Arita, Phys. Rev. B **100**, 205138 (2019).
[14] M. Hirayama, T. Tadano, Y. Nomura, and R. Arita, Phys. Rev. B **101**, 075107 (2020).
[15] P. Jiang, L. Si, Z. Liao, and Z. Zhong, Phys. Rev. B **100**, 201106(R) (2019).
[16] K.-W. Lee and W. E. Pickett, Phys. Rev. B **70**, 165109 (2004).
[17] A. S. Botana and M. R. Norman, Phys. Rev. X **10**, 011024 (2020).
[18] H. Sakakibara, H. Usui, K. Suzuki, T. Kotani, H. Aoki, and K. Kuroki, arXiv:1909.00060.
[19] L.-H. Hu and C. Wu, Phys. Rev. Research **1**, 032046(R) (2019).
[20] X. Wu, D. Di Sante, T. Schwemmer, W. Hanke, H. Y. Hwang, S. Raghu, and R. Thomale, Phys. Rev. B **101**, 060504(R) (2020).
[21] J. Gao, Z. Wang, C. Fang, and H. Weng, arXiv:1909.04657.
[22] M. Jiang, M. Berciu, and G. A. Sawatzky, arXiv:1909.02557.
[23] Z. Liu, Z. Ren, W. Zhu, Z. F. Wang, and J. Yang, arXiv:1912.01332.
[24] P. Werner and S. Hoshino, Phys. Rev. B **101**, 041104(R) (2020).
[25] B. Geisler and R. Pentcheva, arXiv:2001.03762.
[26] F. Bernardini and A. Cano, arXiv:2001.02133.
[27] M.-Y. Choi, K.-W. Lee, and W. E. Pickett, Phys. Rev. B **101**, 020503(R) (2020).
[28] One difference is that Nd has a $4f$ moment and La has not. However, because of the weak hybridization with the Ni-$3d_{x^2-y^2}$, one might expect these to order or undergo a Kondo screening only at prohibitively low temperatures.
[29] T. Katayama, A. Chikamatsu, K. Yamada, K. Shigematsu, T. Onozuka, M. Minohara, H. Kumigashira, E. Ikenaga, and T. Hasegawa, J. Appl. Phys. **120**, 085305 (2016).
[30] T. Onozuka, A. Chikamatsu, T. Katayama, T. Fukumura, and T. Hasegawa, Dalton Trans. **45**, 12114 (2016).
[31] P. Hohenberg and W. Kohn, Phys. Rev. **136**, B864 (1964).
[32] W. Kohn and L. J. Sham, Phys. Rev. **140**, A1133 (1965).
[33] R. M. Martin, *Electronic Structure: Basic Theory and Practical Methods* (Cambridge University Press, Cambridge, England, 2004).
[34] A. Georges, G. Kotliar, W. Krauth, and M. J. Rozenberg, Rev. Mod. Phys. **68**, 13 (1996).
[35] G. Kotliar and D. Vollhardt, Phys. Today No. 3 **57**, 53 (2004).
[36] W. Metzner and D. Vollhardt, Phys. Rev. Lett. **62**, 324 (1989).
[37] K. Held, Adv. Phys. **56**, 829 (2007).
[38] P. Blaha, K. Schwarz, G. Madsen, D. Kvasnicka, and J. Luitz, *An Augmented Plane Wave+Local Orbitals Program for Calculating Crystal Properties* (Technische Universitat Wien, Vienna, 2001).
[39] K. Schwarz, P. Blaha, and G. Madsen, Comput. Phys. Commun. **147**, 71 (2002).
[40] G. Kresse and J. Hafner, Phys. Rev. B **48**, 13115 (1993).
[41] J. P. Perdew, K. Burke, and M. Ernzerhof, Phys. Rev. Lett. **77**, 3865 (1996).
[42] J. P. Perdew, A. Ruzsinszky, G. I. Csonka, O. A. Vydrov, G. E. Scuseria, L. A. Constantin, X. Zhou, and K. Burke, Phys. Rev. Lett. **100**, 136406 (2008).
[43] G. H. Wannier, Phys. Rev. **52**, 191 (1937).
[44] N. Marzari, A. A. Mostofi, J. R. Yates, I. Souza, and D. Vanderbilt, Rev. Mod. Phys. **84**, 1419 (2012).
[45] A. A. Mostofi, J. R. Yates, Y.-S. Lee, I. Souza, D. Vanderbilt, and N. Marzari, Comput. Phys. Commun. **178**, 685 (2008).
[46] J. Kuneš, R. Arita, P. Wissgott, A. Toschi, H. Ikeda, and K. Held, Comput. Phys. Commun. **181**, 1888 (2010).
[47] V. I. Anisimov, J. Zaanen, and O. K. Andersen, Phys. Rev. B **44**, 943 (1991).
[48] See Supplemental Material at http://link.aps.org/supplemental/10.1103/PhysRevLett.124.166402 for additional DFT + U and DMFT results, supporting our conclusions.
[49] T. Miyake and F. Aryasetiawan, Phys. Rev. B **77**, 085122 (2008).
[50] I. A. Nekrasov, K. Held, G. Keller, D. E. Kondakov, T. Pruschke, M. Kollar, O. K. Andersen, V. I. Anisimov, and D. Vollhardt, Phys. Rev. B **73**, 155112 (2006).
[51] G. Lantz, M. Hajlaoui, E. Papalazarou, V. L. R. Jacques, A. Mazzotti, M. Marsi, S. Lupi, M. Amati, L. Gregoratti, L. Si, Z. Zhong, and K. Held, Phys. Rev. Lett. **115**, 236802 (2015).
[52] E. Gull, A. J. Millis, A. I. Lichtenstein, A. N. Rubtsov, M. Troyer, and P. Werner, Rev. Mod. Phys. **83**, 349 (2011).
[53] N. Parragh, A. Toschi, K. Held, and G. Sangiovanni, Phys. Rev. B **86**, 155158 (2012).
[54] M. Wallerberger, A. Hausoel, P. Gunacker, A. Kowalski, N. Parragh, F. Goth, K. Held, and G. Sangiovanni, Comput. Phys. Commun. **235**, 388 (2019).
[55] J. E. Gubernatis, M. Jarrell, R. N. Silver, and D. S. Sivia, Phys. Rev. B **44**, 6011 (1991).
[56] A. W. Sandvik, Phys. Rev. B **57**, 10287 (1998).
[57] T. U. Ito, A. Koda, K. Shimomura, W. Higemoto, T. Matsuzaki, Y. Kobayashi, and H. Kageyama, Phys. Rev. B **95**, 020301(R) (2017).
[58] T. Yajima, A. Kitada, Y. Kobayashi, T. Sakaguchi, G. Bouilly, S. Kasahara, T. Terashima, M. Takano, and H. Kageyama, J. Am. Chem. Soc. **134**, 8782 (2012).
[59] T. Yamamoto and H. Kageyama, Chem. Lett. **42**, 946 (2013).
[60] Hydrogen intercalation has also been reported when CaH_2 reducing further Ruddlesden-Popper oxides [61,62].
[61] L. Jin, M. Batuk, F. K. K. Kirschner, F. Lang, S. J. Blundell, J. Hadermann, and M. A. Hayward, Inorg. Chem. **58**, 14863 (2019).
[62] L. Jin and M. A. Hayward, Angew. Chem., Int. Ed. Engl. **59**, 2076 (2020).
[63] The entropy of $1/2$ H_2 at 500 K is $S = 7.5 \times 10^{-4}$ eV/K [64] corresponding to 0.38 eV. On the other hand, the reduction with CaH_2 might lead to a rather high H_2 pressure; and ABO_2H has a higher entropy than ABO_2. Its Mott insulating spin 1 (see below) yields

$S = k_B \ln(3) = 1 \times 10^{-4}$ eV/K corresponding to 0.05 eV at 500 K; a prospective disorder entropy of say $ABO_2H_{0.5}$ would yield $S = k_B \ln(2) = 0.6 \times 10^{-4}$ eV/K or 0.03 eV at 500 K.

[64] M. W. Chase, *NIST-JANAF Themochemical Tables* (J. Phys. Chem. Ref. Data, Monograph, 1998).

[65] F. Denis Romero, A. Leach, J. S. Möller, F. Foronda, S. J. Blundell, and M. A. Hayward, Angew. Chem., Int. Ed. Engl. **53**, 7556 (2014).

[66] M. Amano Patino, D. Zeng, S. J. Blundell, J. E. McGrady, and M. A. Hayward, Inorg. Chem. **57**, 2890 (2018).

[67] T. Yamamoto, D. Zeng, T. Kawakami, V. Arcisauskaite, K. Yata, M. A. Patino, N. Izumo, J. E. McGrady, H. Kageyama, and M. A. Hayward, Nat. Commun. **8**, 1217 (2017).

[68] M. Hayward, E. Cussen, J. Claridge, M. Bieringer, M. Rosseinsky, C. Kiely, S. Blundell, I. Marshall, and F. Pratt, Science **295**, 1882 (2002).

[69] R. M. Helps, N. H. Rees, and M. A. Hayward, Inorg. Chem. **49**, 11062 (2010).

[70] T. Sakaguchi, Y. Kobayashi, T. Yajima, M. Ohkura, C. Tassel, F. Takeiri, S. Mitsuoka, H. Ohkubo, T. Yamamoto, J. e. Kim *et al.*, Inorg. Chem. **51**, 11371 (2012).

[71] Y. Kobayashi, O. J. Hernandez, T. Sakaguchi, T. Yajima, T. Roisnel, Y. Tsujimoto, M. Morita, Y. Noda, Y. Mogami, A. Kitada *et al.*, Nat. Mater. **11**, 507 (2012).

[72] For $(\mathrm{Sr,Nd})\mathrm{NiO_2}$, we perform (antiferro-)magnetic GGA + U calculations in vasp instead of the nonmagnetic calculations for other ABO_2 systems because (i) $\mathrm{NdNiO_3}$ is experimentally determined to be an antiferromagnetic insulator [1] and (ii) nonmagnetic VASP calculations for $(\mathrm{Sr,Nd})\mathrm{NiO_2}$ hardly converge.

[73] V. I. Anisimov, J. Zaanen, and O. K. Andersen, Phys. Rev. B **44**, 943 (1991).

[74] A. Mercy, J. Bieder, J. Iniguez, and P. Ghosez, Nat. Commun. **8**, 1677 (2017).

[75] B. L. Gyorffy, A. J. Pindor, J. Staunton, G. M. Stocks, and H. Winter, J. Phys. F **15**, 1337 (1985).

[76] J. Varignon, M. N. Grisolia, J. Iniguez, A. Barthelemy, and M. Bibes, npj Quantum Mater. **2**, 21 (2017).

[77] G. Trimarchi, Z. Wang, and A. Zunger, Phys. Rev. B **97**, 035107 (2018).

[78] J. Varignon, M. Bibes, and A. Zunger, Nat. Commun. **10**, 1658 (2019).

[79] J. Varignon, M. Bibes, and A. Zunger, Phys. Rev. B **100**, 035119 (2019).

[80] Appropriate DFT or hybrid functionals may also open band gaps in strongly correlated systems, see, e.g., Refs. [81–87].

[81] J. P. Perdew and A. Zunger, Phys. Rev. B **23**, 5048 (1981).

[82] J. Heyd, G. E. Scuseria, and M. Ernzerhof, J. Chem. Phys. **118**, 8207 (2003).

[83] J. M. Tomczak, K. Haule, T. Miyake, A. Georges, and G. Kotliar, Phys. Rev. B **82**, 085104 (2010).

[84] F. Tran and P. Blaha, Phys. Rev. Lett. **102**, 226401 (2009).

[85] J. W. Furness, Y. Zhang, C. Lane, I. G. Buda, B. Barbiellini, R. S. Markiewicz, A. Bansil, and J. Sun, Commun. Phys. **1**, 11 (2018).

[86] Q. Liu, Q. Yao, Z. A. Kelly, C. M. Pasco, T. M. McQueen, S. Lany, and A. Zunger, Phys. Rev. Lett. **121**, 186402 (2018).

[87] C. Lane, J. W. Furness, I. G. Buda, Y. Zhang, R. S. Markiewicz, B. Barbiellini, J. Sun, and A. Bansil, Phys. Rev. B **98**, 125140 (2018).

[88] S. Ryee, H. Yoon, T. J. Kim, M. Y. Jeong, and M. J. Han, Phys. Rev. B **101**, 064513 (2020).

[89] F. Lechermann, Phys. Rev. B **101**, 081110(R) (2020).

[90] J. Karp, A. S. Botana, M. R. Norman, H. Park, M. Zingl, and A. Millis, arXiv:2001.06441.

[91] For a one- and two-band DMFT calculation, cf. [24,92], respectively.

[92] Y. Gu, S. Zhu, X. Wang, J. Hu, and H. Chen, arXiv:1911.00814.

[93] R. D. Sánchez, M. T. Causa, A. Caneiro, A. Butera, M. Vallet-Regí, M. J. Sayagués, J. González-Calbet, F. García-Sanz, and J. Rivas, Phys. Rev. B **54**, 16574 (1996).

[94] M. Abbate, G. Zampieri, F. Prado, A. Caneiro, J. M. Gonzalez-Calbet, and M. Vallet-Regi, Phys. Rev. B **65**, 155101 (2002).

[95] J. Alonso, M. Martínez-Lope, J. García-Muñoz, and M. Fernández-Díaz, J. Phys. **9**, 6417 (1997).

[96] Let us note that DMFT has been quite helpful for understanding the pnictide physics [97–103].

[97] K. Haule, J. H. Shim, and G. Kotliar, Phys. Rev. Lett. **100**, 226402 (2008).

[98] M. Aichhorn, L. Pourovskii, V. Vildosola, M. Ferrero, O. Parcollet, T. Miyake, A. Georges, and S. Biermann, Phys. Rev. B **80**, 085101 (2009).

[99] V. I. Anisimov, D. M. Korotin, M. A. Korotin, A. V. Kozhevnikov, J. Kuneš, A. O. Shorikov, S. L. Skornyakov, and S. V. Streltsov, J. Phys. Condens. Matter **21**, 075602 (2009).

[100] P. Hansmann, R. Arita, A. Toschi, S. Sakai, G. Sangiovanni, and K. Held, Phys. Rev. Lett. **104**, 197002 (2010).

[101] A. Toschi, R. Arita, P. Hansmann, G. Sangiovanni, and K. Held, Phys. Rev. B **86**, 064411 (2012).

[102] I. A. Nekrasov, N. S. Pavlov, and M. V. Sadovskii, JETP Lett. **102**, 26 (2015).

[103] D. Guterding, S. Backes, M. Tomi, H. O. Jeschke, and R. Valentí, Phys. Status Solidi (b) **254**, 1600164 (2017).

[104] S. Iimura, S. Matsuishi, H. Sato, T. Hanna, Y. Muraba, S. W. Kim, J. E. Kim, M. Takata, and H. Hosono, Nat. Commun. **3**, 943 (2012).

[105] J. Matsumoto, K. Hanzawa, M. Sasase, S. Haindl, T. Katase, H. Hiramatsu, and H. Hosono, Phys. Rev. Mater. **3**, 103401 (2019).

[106] J. Chaloupka and G. Khaliullin, Phys. Rev. Lett. **100**, 016404 (2008).

[107] P. Hansmann, X. Yang, A. Toschi, G. Khaliullin, O. K. Andersen, and K. Held, Phys. Rev. Lett. **103**, 016401 (2009).

[108] P. Hansmann, A. Toschi, X. Yang, O. K. Andersen, and K. Held, Phys. Rev. B **82**, 235123 (2010).

[109] X. Wang, M. J. Han, L. de' Medici, H. Park, C. A. Marianetti, and A. J. Millis, Phys. Rev. B **86**, 195136 (2012).

[110] A. Subedi, O. E. Peil, and A. Georges, Phys. Rev. B **91**, 075128 (2015).

[111] O. Janson and K. Held, Phys. Rev. B **98**, 115118 (2018).

[112] Also in Ref. [9] it has been reported to be difficult to remove the excess oxygen.

[113] M. Hayward, M. Green, M. Rosseinsky, and J. Sloan, J. Am. Chem. Soc. **121**, 8843 (1999).

[114] The hydrogen surplus "fluorite peak" of Ref. [113] has not been detected for the superconducting nickelates in Ref. [1].

[115] K. Lee, B. H. Goodge, D. Li, M. Osada, B. Y. Wang, Y. Cui, L. F. Kourkoutis, and H. Y. Hwang, APL Mater. **8**, 041107 (2020).